Multi-scale tissular-cellular model for wound healing

Luís Almeida, Patrizia Bagnerini

Multi-scale tissular-cellular model for wound healing

Luís Almeida

CNRS, UMR 7598, Laboratoire Jacques-Louis Lions
and UPMC Univ Paris 06, UMR 7598, Laboratoire Jacques-Louis Lions
F-75005, Paris, FRANCE

Patrizia Bagnerini

Dipartimento di Ingegneria Meccanica, Energetica, Gestionale e dei Trasporti
Università degli Studi di Genova
P.le Kennedy-Pad D, 16129 Genova, ITALY

Abstract

In previous works we developed continuous mathematical models for wound healing and dorsal closure in Drosophila embryos. In this paper we extend this study to the case of non convex wounds in Drosophila pupal epithelium where the sign of the local curvature of the boundary plays an important role in determining the type of acto-myosin contractile structure that is formed. Moreover, we propose a multi-scale model where we combine the previous continuous approach with a cellular-level model that also takes into account interfacial tension between cells. We therefore minimize an extended energy functional so that the junctions of the cells are moved through successive configurations in order to obtain a new mechanical equilibrium. We apply this model to study some simple situations of cell sorting and the movement of genetic clones.

1 Introduction

Extension of an epithelial membrane to close a hole is a very widespread process both in morphogenesis and in tissue repair. Contraction of actin structures (in one, two or three dimensions) plays an important role in many cellular and tissue movements, both at a multicellular tissue level and at a cellular (and even intracellular) one: from muscle contraction to cell crawling and the contractile ring in cytokinesis. In the [2], [3], [1] we proposed various mathematical models for simulating the contraction of an actin cable structure attached to an external epithelial tissue in different

Keywords: Actin cable, Wound healing, Dorsal closure, Movement of epithelia, Forces in embryogenesis.

The authors thank the ANR project REGENR for support

applications such as wound healing or dorsal closure in Drosophila Melanogaster (fruit fly) embryos.

The present work is a natural sequel of these works, but here we are more concerned with wound healing in the pupal stage of Drosophila. An interesting feature of this stage is that the epidermis is under considerably less tension than in embryos. This enables us to make holes which do not become convex while they open, differently to embryo experiments where the the strong pull of the external epidermis renders the hole convex during the opening phase.

In particular, in collaboration with A. Jacinto's lab (CEDOC, Universidade Nova de Lisboa), we generated C-shaped wounds, where part of the boundary is concave and the rest convex (see figure 1). Observing the healing of this type of wound, we realized that the parts of the boundary where the curvature is positive and those where it is negative don't behave in the same way (see also the discussion in [5]). We propose here (in section 2) to extend the previous model to describe and simulate this phenomenon. Then, in section 3, we couple the continuum model with a cellular one, where the epidermal tissue is described by a two-dimensional network of cells interacting through their common boundaries.

There are many different cell types in multicellular organisms that result from differentiation from embryo stem cells (through specific gene expression) as part of tissue specialization mechanisms: during morphogenesis cells are separated into compartments that are essential for proper assembly of the body's organs. Inside these compartments, once differentiated, cells are usually committed to a particular lineage and cells belonging to each compartment stay together and do not mix with those from other compartments. Cell sorting is therefore an interesting and open problem. Two main hypothesis have been formulated: first, cell segregation at compartment boundaries could be based on *differential cell adhesion* or affinity (i.e. cell populations might develop distinct adhesive properties which prevent intermingling), but molecules involved in these processes have still not been completely identified. The second hypothesis is the *differential interfacial tension* i.e. cells in contact with neighboring cells of a different type, increase the tension at the interfaces and contract the corresponding surfaces.

Motivated by these problems and by some experiences in collaboration with A. Jacinto (work in progress), we consider the tissue formed by a group of cells of two different types, for instance wild type ones and others that are mutant for a certain gene. In section 4, in order to take into account the difference in the interfacial tension between cells of different types, we introduce in the continuum-cellular model an extended energy functional. The junctions of the cells are then moved through successive configurations minimizing this functional in order to obtain a new mechanical equilibrium at each step.

2 C-shaped wounds in Drosophila pupae

In the few minutes that follow a laser (or a mechanical) circular wounding of the epidermis filamentous actin and myosin II concentrate inside the adjacent cells and give rise to a local acto-myosin cable anchored to the adherens junctions that bind the cell to its neighbors. The result is a continuous, supracellular acto-myosin cable that encircles the wound and reduces the wound's perimeter by a purse-string mechanism. In the (not yet published) experiences in collaboration with A. Jacinto's lab, in the C-shaped wounds on pupae, the acto-myosin cable seems to form mainly on the part of the boundary where the curvature is positive. For this reason, in our model the contractile actin cable term is given by $\max(\kappa, 0)$, where κ represents the curvature.

In [4], the authors considered the question of arbitrarily shaped wounds from a theoretical point of view: denoting by $E(t)$ (a subset of $\mathbb{R}^2$) the position of the wound at time t, they study $C^{1,1}$ solutions of the formal geometric equation

$$V(x) = \begin{cases} \kappa(x) & \text{if } x \in \Omega \\ \max(\kappa(x), 0) & \text{if } x \in \partial\Omega \end{cases} \tag{1}$$

where κ denotes the curvature of a closed curves $\partial E(t) \subset \mathbb{R}^2$ (boundaries of the sets $E(t)$) and V the normal inward velocity (i.e. pointing inside $E(t)$). They prove that the solution $E(t)$ of the mean curvature flow with obstacle is contained at each time t in the corresponding solution of the unconstrained mean curvature flow starting from the same set $E(0)$. In the context of our original biological problem and the proposed models, this result indicates that the strategy of assembling an acto-myosin cable only in the positive curvature part of the boundary of the wound (or hole) allows us close it in a more efficient way than if we had assembled the cable all around the boundary.

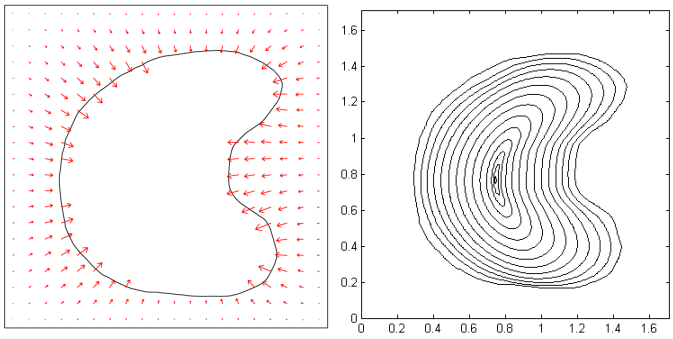

Figure 1: The initial wound is a C-shaped curve in the domain [0, 1.7]x[0, 1.7]. We show in the left part of the figure the vector field u_i solution of problem (2) at the initial step $i = 1$ with $f_{cable} = 0.05$ and $f_{pull} = 0$. In the right part we show the successive curve positions.

Flowing only by the positive part of the curvature corresponds (see [4]) to the special case of problem (1) where the obstacle is taken to be the initial position of the boundary. Another nice feature of this type of flow having a natural biological interpretation is the fact that, during the wound closure phase, the epidermis advances without ever retreating, even locally or temporarily, from a region it has occupied (which would not be always true for a full curvature flow corresponding to having assembled a cable all around the wound closure).

In adult wounds, the main closure mechanism is lamellipodial crawling, i.e. the cells in the first rows extend lamellipodia (which are essentially two dimensional actin structures) that attach to extracellular matrix and pull the epithelium forward into the wounded area. Beneath, at the dermal level, activated fibroblasts proliferate and give rise to the granulation tissue which actively contracts. Both these contributions will be taken into account in the model by introducing in the equation (2) the term $f_{pull}\,\mathbf{n}$, i.e. an active pull (of the lamellipodia or the connective tissue) on the leading edge that moves it inwards to close the hole.

For epidermal wounds and the morphogenetic movements that we consider, the time scale of the closure is very long (hours) while the space scale is very small (cell characteristic length - of the order of a few μm). Therefore, it is reasonable to, in a first approximation, neglect inertial forces, and assume that the dynamic process of wound closure is a succession of static equilibria, i.e. to do a quasi-static approximation.

Taking into account the previous discussion, we propose the following quasistatic model: we consider as simulation domain a rectangle M, which contains the wound at time step i, denoted by W_i. Let D_i be the part of the domain occupied by the epidermis i.e. $D_i = M \setminus W_i$ and $\omega_i = \partial W_i$ the boundary of the wound ("the leading edge"). The acto-myosin cable tension gives rise to a force that is proportional to the curvature. This term will be described by a normal force which is proportional to the local curvature of the leading edge at each point. It points towards the interior of the wound W_i at the points of positive curvature and towards the exterior at points of negative curvature. We assume that at each time step i, the corresponding displacement field $\mathbf{u}_i$ satisfies

$$\begin{cases} -\Delta \mathbf{u}_i = \mathbf{0} \ \text{ in } \ D_i, \\ \mathbf{u}_i = \mathbf{0} \ \text{ on } \partial M, \\ \dfrac{\partial \mathbf{u}_i}{\partial n} = f_{cable}\ \max(\kappa, 0)\,\mathbf{n} + f_{pull}\,\mathbf{n} \ \text{ on } \omega_i\ . \end{cases} \tag{2}$$

where $\mathbf{n}$ is the external unit normal to ∂D_i at each point, κ the curvature, f_{cable} the function associated with the intensity of the cable tension at each point along the leading edge ω_i and f_{pull} is function describing the intensity of the inwards pull (of the filopodia/lamellipodia or the connective tissue). We use bold face letters for $\mathbf{u}_i$, $\mathbf{n}$ and $\mathbf{0}$ to make it clear that all these quantities are vectors. We choose Dirichlet homogeneous boundary condition on the boundary of the rectangle M, since, differently from embryos, in the pupae stage epidermis is not under a significant tension and the tissue can be considered at equilibrium.

The algorithm is the following. First we compute the solution of problem (2) in the domain $D_i = M \backslash W_i$ by using finite element methods on a triangular mesh (using Comsol Multiphysics software). We obtain in this way a displacement field $\mathbf{u}_i$. Then, we extended it to the domain inside the inner boundary ω_i by solving

$$\begin{cases} -\Delta \mathbf{u}_i^{int} = 0 \ \text{ in } \ W_i, \\ \mathbf{u}_i^{int} = \mathbf{u}_i \ \text{ on } \omega_i. \end{cases} \tag{3}$$

We obtain in this way an extension (the harmonic extension) of the original vector field $\mathbf{u}_i$ (which for simplicity we will still denote by $\mathbf{u}_i$) defined on rectangular domain M. In order to perform the evolution of contour ω_i, we use level set methods. They consist in implicitly representing the front ω_i as the zero level set of a function $\Phi : \mathbb{R}^2 \times \mathbb{R}^+ \to \mathbb{R}$, solution of the Hamilton-Jacobi equation (HJ)

$$\begin{cases} \partial_t \Phi(x,t) + \mathbf{u}_i(x) \cdot \nabla \Phi(x,t) = 0 \ \text{ in } \ M \times [0,T], \\ \Phi(x,0) = \Phi_i(x) \ \text{ in } \ M, \end{cases} \tag{4}$$

where $\mathbf{u}_i$ (solution of our original problem extended using (3)) gives the direction of front propagation and ∇ denotes the spatial gradient. For the first step, the function $\Phi_1(x)$ is obtained by computing the signed distance to the initial contour ω_1 (positive at the interior of ω_1), whereas for the following contours, $\Phi_i(x)$ is the solution of (4) computed at the previous time step $i-1$.

We use an Eulerian method instead of a particle (Lagrangian) method since changes of topology are naturally handled and surfaces automatically merge and separate. We solve the HJ problem (4) on a regular cartesian grid by using an upwind second order Essentially Non-Oscillatory (ENO) scheme in space and a second order total variation diminishing Runge-Kutta scheme in time. The value of $\mathbf{u}_i$ in the regular grid is computed by interpolating $\mathbf{u}_i$ on a triangular mesh. The level set methods are implemented by using the Matlab toolbox of I. M. Mitchell ([10]).

Since we are doing a quasistatic analysis, the time scale is free for us to fix and thus the numeric values of coefficients f_{cable} and f_{pull} are not physically significant - just the relative values of the different coefficients make a difference in the simulations (up to rescaling time). To have an idea of size and dynamics of the real situation, small wounds with a diameter of a few tens of μm close in a couple of hours. We choose a time interval T in problem (2) (to pass from the time step i to the time step $i+1$) equal to 0.1 and a spatial discretization step equal to 0.1 both in x and y directions.

The numerical experiment shown in figure 1 corresponds to the successive positions of the boundary ω_i with constant cable tension $f_{cable}(q,i) = 0.2, \forall i = 1 \dots N, \ \forall q \in \omega_i$ and null lamellipodial force $f_{pull} = 0$. We notice that, for simplicity, we do not consider a time dependence (where time is the index i as described before) of the values of the different terms, but the model allows such dependence.

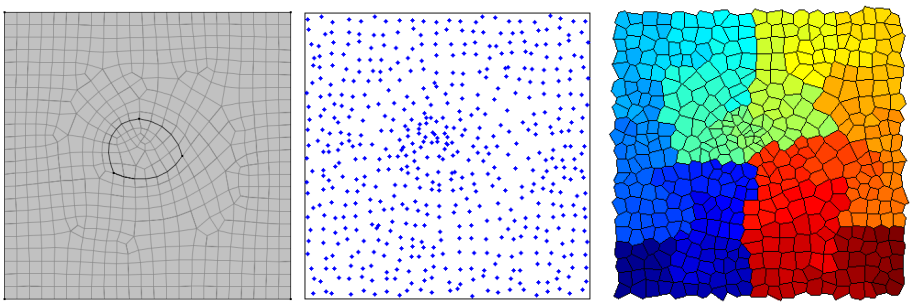

Figure 2: Generation of the initial configuration: from the left to the right we show resp. the quadrilateral mesh, the barycenter of the element of the mesh after jiggle and the Voronoi diagram of these points.

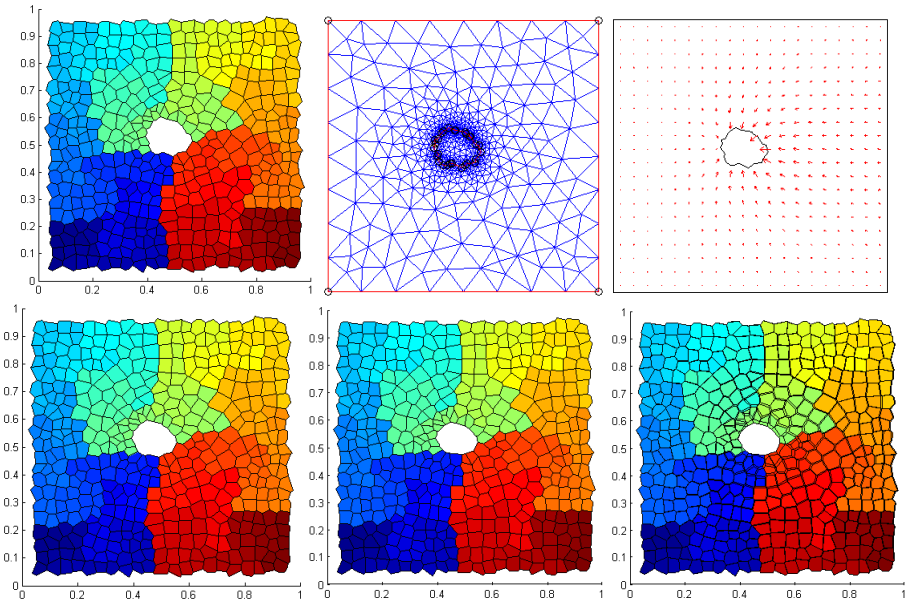

Figure 3: Coupling of continuum-cellular model: first row, left to right: the initial configuration, the mesh used to compute the solution of (2) and the corresponding displacement field $\mathbf{u}_i$ at time step i.; second row, left to right: the cells at two successive equilibrium time step and the difference of cells between two successive times.

3 Multiscale continuum-cellular model

The model presented above is a macroscopic model that does not take into account the positions of the individual cells constituting each of the tissues considered. It provides a description at a tissue-level space scale and, being a continuous model, has no ambition of describing the changes in geometry of individual cells - for such a detailed description the geometry of each cell and its neighbors should also play an important role.

Therefore, we decided to couple the continuum model with a cellular one. When the number of cells in the tissue is big, people often concentrate on a small group of cells, not being able to follow in detail all the cells in the system. In this situation, the macroscopic models can be useful for providing reasonable boundary or asymptotic conditions for the cellular-level studies. Moreover, the displacement field $\mathbf{u}_i$ solution of problem (2) can be used to move the junctions of the cells of the tissue. Like in [6, 9, 7], we represent the epidermal tissue as a two-dimensional network of cells discretized as polygons and interacting through their common boundaries (modeled as straight lines connecting vertices).

To perform simulations and test the model, we need to generate a certain number of initial cell configurations. To achieve this, we first generate a quadrilateral mesh in the domain and we compute the barycenters of each elements of the mesh. Next, we jiggle the barycenters of a small random quantity and then we construct the Voronoi triangulation of these points. We choose this procedure to take advantage of the capabilities of mesh generators to obtain elements of the desired size, stretched in one direction, etc.

Let $P(i)$ be the vertices of the cells of the epidermal tissue included in D_i at time step i. We displace the set of points $P(i)$ (belonging to ω_i) by using the vector field $\mathbf{u}_i$ in order to obtain a new set of points $P(i+1)$ belonging to D_{i+1}, i.e. the vertices of the cells at the following time. Let $\mathbf{p}_j(i) = (x_j(i), y_j(i))$, $j = 1, \dots N$ be the coordinates of the points of the set $P(i)$ at time step i. We compute the coordinates $\mathbf{p}_j^{i+1}$ of the points in $P(i+1)$ at time step $i+1$ by solving (with a fourth order Runge-Kutta scheme) for each of them, the following boundary value problem (we will be solving this problem N times, with a different initial condition for each j)

$$\begin{cases} \mathbf{p}'(t) = \mathbf{u}_i \ \text{ in } \ [0,T] \\ \mathbf{p}(0) = \mathbf{p}_j(i) = (x_j^i, y_j^i). \end{cases} \tag{5}$$

4 Cell sorting and genetic clones

We already studied cell segregation in [8]. By studying the cellular tension in Drosophila Dorsal Closure (a stage of embryo development), we realized that there were some cells at the segment boundaries (which we called *mixer* or *chameleon* cells) with a very peculiar and previously not described behavior: they change their genetic identity making a transdifferentiation. Consequently, they do not respect

compartment boundaries and give rise to unexpected cell rearrangements at the leading edge.

Motivated by this work and by some experiences on wound healing on Drosophila pupae in collaboration with A. Jacinto (currently in progress), we consider in the tissue a group of cells of different type, i.e. for instance, mutant for a certain gene. Another possible application is the clones in the wing imaginal disc. Like in the segmentation of Drosophila embryos epithelia, wing disc contains a compartment boundary that separates anterior (A) from posterior (P) cells. This compartment boundary is under the control of the secreted protein Hedgehog (Hh), even thought the precise mechanism remains poorly understood. In [6] they generate cells that lost the ability to transduce the Hh signal (becoming mutant for that gene). Clones in the posterior (P) compartment have wiggly borders with their neighbors since neither cells of the clone nor cells in its neighborhood transduce the Hh signal (cells marked "off" in figure 4). In contrast, clones (arrowhead) have smooth borders when situated in the anterior (A) compartment, since cells surrounding the clone respond to the Hh signal (cells marked "on" in figure 4) and therefore clones try to minimize their surface contact with the neighboring cells. The large clone in the middle is of anterior origin and has taken up a position in the posterior segment. Aiming at studying cell sorting at compartment boundaries, we introduce in the continuum-cellular model the possibility to modify the interfacial tension between cells of different types.

The algorithm is the following. At each time step i, we compute the solution of the continuum model, i.e. the displacement field $\mathbf{u}_i$. Second, we move the junctions of the cells by solving the system of ordinary differential equation (5). Then, we take into account the difference in the interfacial tension between cells of different types, leading the cells to go through successive configurations in order to obtain a new mechanical equilibrium at each step. Stationary and stable network configurations satisfy a mechanical force balance, i.e. at each junction, the sum of forces vanish. We describe these force balances as local minima of an energy function. So, we compute a new stable network configuration by minimizing the following functional (P represents the cell configuration which is defined by the set of the vertices of all the cells, and α is the cell index):

$$F(P) = \sum_{\alpha=1}^{N_C} \sum_{<mn>} \Lambda_{mn} l_{<mn>} + \sum_{\alpha=1}^{N_C} \frac{K}{2}(A_\alpha - \bar{A}_\alpha)^2 + \sum_{\alpha=1}^{N_C} \frac{\Gamma}{2} L_\alpha^2, \tag{6}$$

The first term describes the contributions due to the line tension along each of the edges $< mn >$ (between vertices m and n) of each cell α, the second one to cell area elasticity, and the third one the elasticity of the cell perimeter. The parameter N_C is the number of cells where we perform minimization (it can be a subset of the total cells of the tissue), $l_{<mn>}$ is the edge length, L_α the perimeter of cell α, $\bar{A}_\alpha$ the preferred area (the actual area of the cell at time step i) and Λ_{mn} the line tension on edge $l_{<mn>}$ depending on the gradient in the tension. We obtain in this way a new cell configuration at time step $i+1$. The minimization of the functional

F of (6) is performed using the Matlab function fminsearch. In figure 4 we show the result of the simulation. As expected, the clone becomes round, since it minimizes its contact surface with its neighboring cells (which are genetically different).

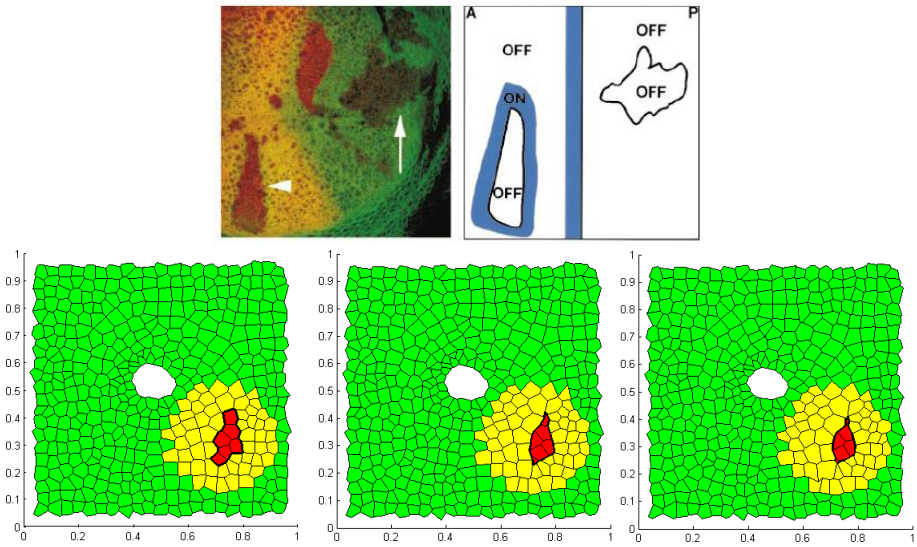

Figure 4: First row: the image is taken from [6]. Clones in the posterior (P) compartment have wiggly borders with their neighbors since neither cells of the clone nor cells in its neighborhood transduce the Hh signal (cells marked "off"). In contrast, clones (arrowhead) have smooth borders when situated in the anterior (A) compartment, since cells surrounding the clone respond to the Hh signal (cells marked "on") and therefore try to minimize their surface contact with the neighboring cells. Second row, left to right: the simulation of the movement of the clone at successive time steps.

References

[1] Almeida, L.; Bagnerini, P.; Habbal, A.; Noselli, S. and Serman, F. *A mathematical model for dorsal closure*, J Theor Biol, **268** (2011), 105-119.

[2] Almeida, L.; Bagnerini, P.; Habbal, A.; Noselli, S. and Serman, F. *Tissue repair modeling*, Singularities in nonlinear evolution phenomena and applications, Ed. Norm., Pisa, **9** (2009), 27-46.

[3] Almeida, L.; Bagnerini, P. and Habbal, A. *Modeling actin cable contraction*, Comput. Math. Appl., **64** (2012), 310-321.

[4] Almeida, L.; Chambolle, A. and Novaga, M.. *Implicit scheme for mean curvature flow with obstacles*, Annales de l'Institut Henri Poincare (C) Non Linear Analysis, **29** (2012), 667 – 681.

[5] Almeida, L.; Demongeot, J.. *Predictive power of "a minima" models in biology*, Acta Bioth., **60** (2012), 3–19.

[6] C Dahmann and K Basler. *Opposing transcriptional outputs of hedgehog signaling and engrailed control compartmental cell sorting at the drosophila a/p boundary*, Cell, **100(4)** (2000), 411-422.

[7] R. Farhadifar, J. Röper, B. Aigouy, S. Eaton, and F. Jülicher. *The infuence of cell mechanics, cell-cell interactions, and proliferation on epithelial packing*, Curr Biol, **17(24)** (2007), 2095-2104.

[8] Gettings, M.; Serman, F.; Rousset, R.; Bagnerini, P.; Almeida, L. and Noselli, S. *JNK signalling controls remodelling of the segment boundary through cell reprogramming during Drosophila morphogenesis*, PLoS Biol, **8** (2010).

[9] T. Lecuit and P. Lenne. *Cell surface mechanics and the control of cell shape, tissue patterns and morphogenesis*, Nat Rev Mol Cell Biol, **8(8)** (2007), 633-644.

[10] Mitchell, I. M.. *The flexible, extensible and efficient toolbox of level set methods*, J. Sci. Comput., **35** (2008), 300-329.